

High pressure regime of plasma enhanced deposition of microcrystalline silicon

E. Amanatides, A. Hammad, E. Katsia, and D. Mataras^{a)}

Department of Chemical Engineering, Plasma Technology Laboratory, University of Patras, P.O. Box 1407, 26504 Patras, Greece

(Received 10 August 2004; accepted 18 January 2005; published online 22 March 2005)

An investigation of the effect of the total gas pressure on the deposition of microcrystalline thin films from highly diluted silane in hydrogen discharges was carried out at two different frequencies. The study was performed in conditions of constant power dissipation and constant silane partial pressure in the discharge while using a series of plasma diagnostics as electrical, optical, mass spectrometric, and *in situ* deposition rate measurements together with a simulator of the gas phase and the surface chemistry of SiH₄/H₂ discharges. The results show that both the electron density and energy are affected by the change of the total pressure and the frequency. This in turn influences the rate of high energy electron-SiH₄ dissociative processes and the total SiH₄ consumption, which are favored by the frequency increase for most of the pressures. Furthermore, frequency was found to have the weakest effect on the deposition rate that was enhanced at 27.12 MHz only for the lowest pressure of 1 Torr. On the other hand, the increase of pressure from 1 to 10 Torr has led to an optimum of the deposition rate recorded at 2.5 Torr for both frequencies. This maximum is achieved when the rate of SiH₄ dissociation to free radical is rather high; the flux of species is not significantly hindered by the increase of pressure and the secondary gas phase reactions of SiH₄ act mainly as an additional source of film precursors. © 2005 American Institute of Physics. [DOI: 10.1063/1.1866477]

I. INTRODUCTION

The application of hydrogenated microcrystalline silicon ($\mu\text{c-Si:H}$) in single junction or tandem devices during the last decade, has demonstrated a promising potential for stable, high-efficiency, and cost-effective thin-film solar cells.¹⁻⁴ The intrinsic material is typically deposited at relatively low rates from highly diluted silane in hydrogen rf discharges. The key obstacle for generalizing the use $\mu\text{c-Si:H}$ is still, primarily for economical reasons, the need for higher absorbing layer thicknesses^{5,6} which imposes growth at much higher rates while maintaining the film quality.^{7,8}

The results of the continuing research efforts have clarified so far that both the properties and the growth rate are affected by the variation of the partial pressure of silane,⁹ the interelectrode distance,¹⁰ the rf power,¹¹ the excitation frequency,¹² and the total gas pressure.¹³ Among these, the increase of frequency and pressure were found to have a stronger effect on the growth rate.

In particular, the increase of the excitation frequency from 13.56 MHz to very high frequency (vhf) was found to have a beneficial effect on the deposition rate without significantly affecting the film properties.¹⁴⁻²⁰ This has led to a number of theoretical and experimental studies focused on the effects of frequency on the plasma structure,²¹ the ion and electron kinetics,²² the electron energy distribution function (eedf),²³ the power dissipation,²⁴ and the production of radicals through electron-molecule collisions.²⁵ Through these investigations it is now quite well understood that the

increase of frequency enhances the electron density and increases the SiH₄ dissociation rate towards free radicals, thus increasing the film precursor fluxes towards the surfaces.^{19,25} The high crystalline volume fraction observed in films deposited at higher frequencies is attributed to the hydrogen atom flux towards the substrate which increases for similar reasons.¹⁹

On the other hand, the increase of the total gas pressure above 1 Torr, initially proposed by Guo *et al.*,²⁶ is also being intensely investigated by several groups.²⁷⁻³⁵ It has been shown that it is possible to deposit device grade $\mu\text{c-Si:H}$ thin films at deposition rates as high as 15 Å/s even at the conventional frequency of 13.56 MHz,¹³ while recent results have demonstrated high efficiency devices with $\mu\text{c-Si:H}$ layers deposited at the pressure of 10 Torr.^{36,37} These studies include interpretations of the beneficial effect of pressure on the film growth rate and crystallinity based on “expected” changes like the enhancement of silane consumption (depletion), the high hydrogen atom flux to the surfaces and the reduction of ion bombardment under these conditions.^{13,35} However, there is no experimental or theoretical evidence to support or quantify these “logical” assumptions. As an example, although the high pressure regime is often called the “high pressure silane depletion technique” no experimental measurements of SiH₄ consumption are usually reported in the relevant publications.

It is obvious from this discussion that there is a need for further experimental and theoretical work for understanding the basic changes that do occur in reality in this high pressure regime, in order to be able to exploit its limits. In this direction, the present work has three main goals: First, to

^{a)}Author to whom correspondence should be addressed; electronic mail: dim@plasmatech.gr

investigate the effect of the total gas pressure increase on the SiH_4/H_2 discharge properties and the film growth rate. Second, to study the specific importance of the increase of either the rf frequency or the total gas pressure on the same parameters, and while finally the third goal is to see if a combination of frequency and pressure increase can be beneficial. In order to accomplish these goals, special attention is focused on isolating as much as possible the true effect of frequency and pressure on the deposition process from other possibly interfering discharge parameters. This is achieved by performing all the experiments in conditions of constant rf power consumption in the discharge and at the same time with constant silane partial pressure. The process is investigated by a set of plasma diagnostics including Fourier transform power and impedance analysis (FTPIA), spatially resolved emission spectroscopy (SRES), mass spectrometry and laser reflectance interferometry (LRI), together with an extended simulator of the gas phase and the surface processes. The experimental measurements and the model results are then used to examine the effect of pressure and frequency on the electron density and energy, the rate of electron-induced SiH_4 dissociation, the total SiH_4 conversion, the species mass transport to the deposition surface, and finally the film growth rate. These results are further discussed and compared against literature findings.

II. EXPERIMENT

The measurements were performed in a capacitively coupled ultrahigh vacuum parallel plate reactor, having a base vacuum of 10^{-9} mbar at 250°C . The 120 mm in diameter rf electrode is fixed to the chamber while the 90 mm grounded (deposition) electrode can be freely moved to vary the interelectrode spacing (d).

The amount of rf power actually fed into the discharge chamber is determined using an accurate method employing Fourier transform analysis of power and phase from acquired current and voltage measurements. Namely, the rf voltage and the discharge current wave forms are measured on the powered electrode lead, using a high impedance 1:100 attenuation voltage probe and a $0.1\ \Omega$ transfer impedance rf current probe, and then processed as described in Ref. 38. Different sets of electrical measurements were initially performed to determine the rf voltages leading to constant power dissipation in the discharge throughout the range of all the conditions examined here.

Mass spectrometric measurements were performed using a hidden analytical (HAL 301) quadrupole mass spectrometer connected at the exhaust port of the reactor. The gas sampled, through a variable leak valve in a smaller sampling chamber was analyzed after 70 eV electron impact ionization and the partial pressure of SiH_4 in the reactor was determined by measuring the ion currents $I(m/e)$ at $m/e=30$, 31, and 32. The method used for calibration and transformation of the measured ion currents in the sampling chamber to actual SiH_4 partial pressures in the reactor is described elsewhere.³⁹

Axial emission intensity distribution profiles of excited radicals in the interelectrode space were recorded as de-

scribed in Ref. 40. The difference here is that the optical system, consisting of two slits and an optical fiber manifold equipped with collimating and focusing optics, is moved instead of moving the reactor. The spatial resolution is better than 0.1 mm which is more than enough for detecting all the characteristic features of the emission profiles.

The $\mu\text{c-Si:H}$ films with a typical $2\ \mu\text{m}$ thickness, were grown on Corning 7059 at a substrate temperature of 250°C using electronic quality gases that were further purified. The deposition rate was measured *in situ* using LRI.⁴¹ Moreover, powder suppression techniques were used together with laser light scattering to ensure that the measurements are made in dust free conditions. In this direction, a relatively high total flow rate of 400 sccm and heating of the reactor walls were used. Constant silane partial pressure was assured by using accurate mass flow measurements while the pressure was controlled independently from flow using a baratron gauge and a downstream throttle valve controller before the roots blower.

III. RESULTS

A possible approach for isolating the effect of the total pressure on the microcrystalline silicon deposition process is to keep constant the other possibly interfering discharge parameters. Among these, SiH_4 concentration and discharge power are the most critical and can be strongly affected by the increase of pressure. Namely, the increase of pressure normally increases SiH_4 concentration in the reactor if one compares discharges with the same SiH_4/H_2 flow ratio. Moreover, the increase of pressure leads to higher power consumption if either the voltage or the generator output power is maintained constant, due to an increase of the electron–molecule collision frequency and a more efficient power coupling respectively.³⁸ Experimentally, the constant silane partial pressure (0.025 Torr) was achieved by reducing the fraction of SiH_4 in H_2 from 2.5% to 0.25% as the total pressure was increased, with a step of 2.5 Torr, from 1 to 10 Torr. On the other hand, constant power consumption in the discharge ($8\ \text{W}/72\ \text{mW}/\text{cm}^2$) was achieved by adjusting the rf voltage while performing FTPIA as described in the Sec. II.

Two sets of experiments were carried out, one at the usual 13.56 MHz frequency and one at 27.12 MHz, which can be easily adopted in industrial processes with only minor modifications. At each frequency and pressure, five electrode gaps (from 10 to 25 mm) were scanned, in order to examine the effect of these two parameters at different discharge geometries. However, in this work only the $d=15$ mm measurements are presented, mainly because this is the electrode gap that optimizes the deposition rate independent of frequency and pressure. In addition, the effect of the electrode gap on the deposition rate is discussed in Sec. III C, while more details concerning the combined effect of pressure and electrode gap can be found in Ref. 42.

A. Electrical measurements

As already mentioned, the electrical conditions ensuring constant power consumption in the discharge were deter-

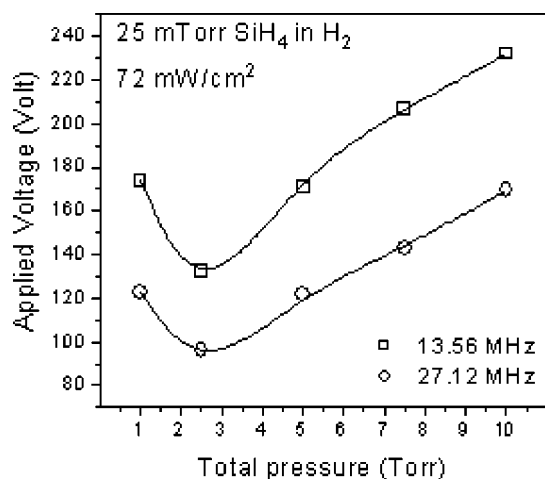


FIG. 1. rf voltage amplitude as a function of the total gas pressure for the frequencies of 13.56 and 27.12 MHz.

mined by performing many different sets of measurements at each pressure, frequency, and electrode gap. The specific power level was chosen as being the upper limit of capacitive discharge operation for the examined range of conditions in our system. Figure 1 presents the results concerning the variation of the rf voltage, necessary for achieving constant 8 W power consumption, as a function of the total pressure. It is observed that a drop of the rf voltage is required as the pressure increases from 1 to 2.5 Torr. Further increase of pressure up to 10 Torr leads to a continuous increase of the voltage. This behavior and the pressure where the minimum required voltage appears, is the same for both frequencies. However, when increasing the frequency to 27.12 MHz, the voltage required for the same power drops significantly ($\sim 30\%$). This result is compatible with previous studies of the effect of frequency dealing with lower pressures.^{24,43,44}

Figure 2 shows the total current flow through the discharge as a function of the gas pressure at the conditions of Fig. 1. The discharge current drops with increasing pressure at both frequencies. This drop is very steep from 1 to 2.5 Torr for 27.12 MHz and from 1 to 5 Torr for 13.56 MHz. With regard to the effect of frequency, there is a pressure region around 2.5 Torr where it appears to have almost no effect on plasma conductivity. In all the other pressures (1, 5, 7.5, and 10 Torr) the current is higher at 27.12 MHz compared to 13.56 MHz, which is characteristic of the increase of frequency^{24,45} and in agreement with the results concerning the voltage (Fig. 1).

Moreover, as shown in Fig. 3, the discharge impedance phase at both frequencies becomes less negative at higher pressures. As with current, most changes are observed from 1 to 2.5 Torr for 27.12 MHz and from 1 to 5 Torr for 13.56 MHz. In addition, the increase of frequency generally leads to more resistive discharges except for the 1 Torr case. It is worth observing that above 5 Torr the 27.12 MHz discharges behave as almost pure ohmic loads.

B. Spatially resolved emission

Spatially resolved measurements of the spontaneous emission of silylidene (SiH^* , $A^2\Delta-X^2\Pi$) radicals were re-

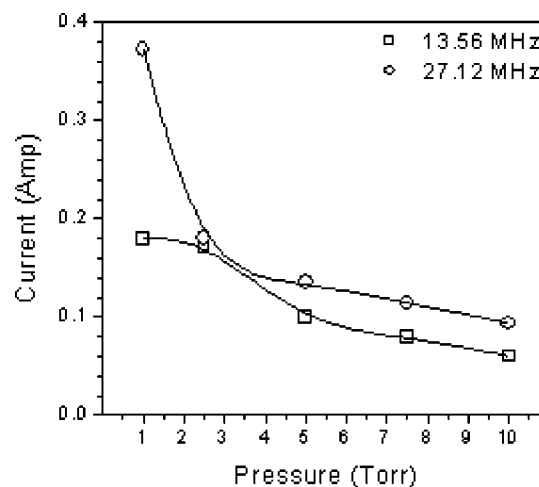


FIG. 2. Total discharge current as a function of the total gas pressure for the frequencies of 13.56 and 27.12 MHz.

corded between the two electrodes in the conditions described above. SiH^* is produced via one-electron impact dissociative excitation of SiH_4 with an energy threshold of 10.5 eV.⁴⁶ The lifetime of these species is 20 ns,⁴⁷ which is quite short compared to the collision time (~ 50 ns) of the species with the background gas mixture up to the pressure of 5 Torr. For higher pressures (7.5 and 10 Torr) the collision time becomes comparable to the de-excitation rate and thus quenching is possible. Therefore, SRES can be a sensitive tool for the investigation of the effect of pressure on the average species' production efficiency of the discharge (up to 5 Torr) as well as for identifying the spatial distribution of the production of species (at all pressures).

Thus, Figs. 4(a) and 4(b) present the normalized axial distribution of SiH^* emission in space for 13.56 and 27.12 MHz and for two pressures (2.5 and 10 Torr), respectively. In the case of 2.5 Torr and 13.56 MHz [Fig. 4(a)], the maximum rate of SiH^* production is located 6 mm from the rf electrode, indicating that rf electrode sheath ohmic heating in the main mechanism of electron energy gain. This is also true for the 27.12 MHz 2.5 Torr case, the only difference being that the maximum is displaced closer to the rf elec-

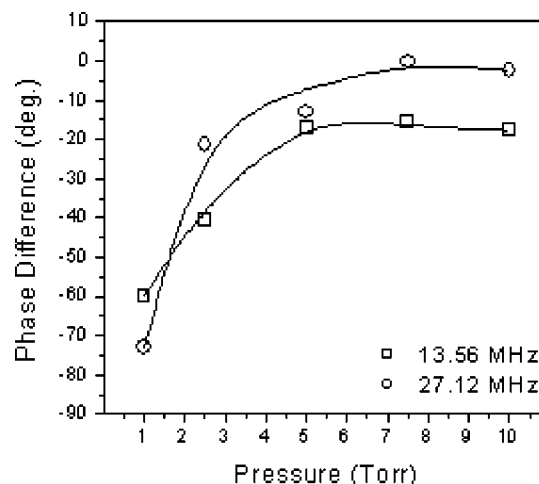


FIG. 3. Discharge phase impedance as a function of the total gas pressure for the frequencies of 13.56 and 27.12 MHz.

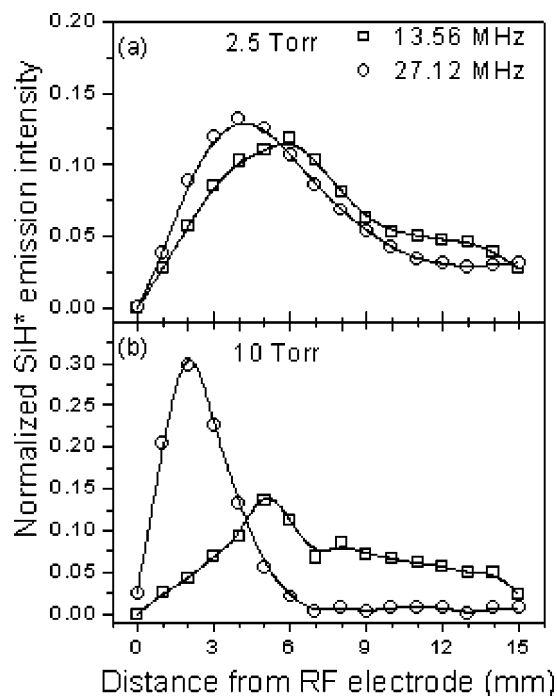


FIG. 4. Spatial distribution of SiH^* ($A^2\Delta-X^2\Pi$) emission intensity for: (a) 2.5 Torr and (b) 10 Torr for the frequencies of 13.56 and 27.12 MHz.

trode (4 mm), in agreement with the decrease of the sheath length with frequency that is mainly due to the increase of the plasma density.^{24,43} On the other hand, at 10 Torr 13.56 MHz [Fig. 4(b)], the observed differences with the respective 2.5 Torr curve are small and only the location of the maximum is slightly displaced from 6 to 5 mm, depicting the expected decrease of the sheath length with pressure. On the other hand, at 10 Torr 27.12 MHz a quite different distribution is recorded. A very steep maximum is now observed very close to the rf electrode (2 mm) while almost no emission is recorded from distances greater than 7 mm. This indicates that at this frequency and pressure, the discharge can be maintained by localized rf electrode sheath heating only because of the significant reduction of charge losses to the electrodes.

Furthermore, the excited species' production efficiency in these conditions is presented in Fig. 5 which shows the total SiH^* emission intensity, calculated by integrating the emission distribution profiles in space, as a function of the pressure for the two frequencies. The total SiH^* production at 13.56 MHz drops continuously with increasing pressure except for the 10 Torr case, where a slight enhancement is observed. However, as mentioned, this observation is valid only up to 5 Torr, whereas quenching must be considered at higher pressures. On the other hand, at 27.12 MHz there is a clear maximum of the total emission intensity located at 2.5 Torr. In this case, further increase of the pressure leads to a reduction of SiH^* intensity even at 10 Torr. It is worth noting that similar observations were reported in previous studies concerning the effect of pressure on the production of excited species.^{13,26,27,33} In two studies,^{13,33} the optimum was observed at 4 Torr, while in the other works^{26,27} at about 1.5 Torr. Most of the authors attributed this behavior to an advantageous balance between the SiH_4 partial pressure and

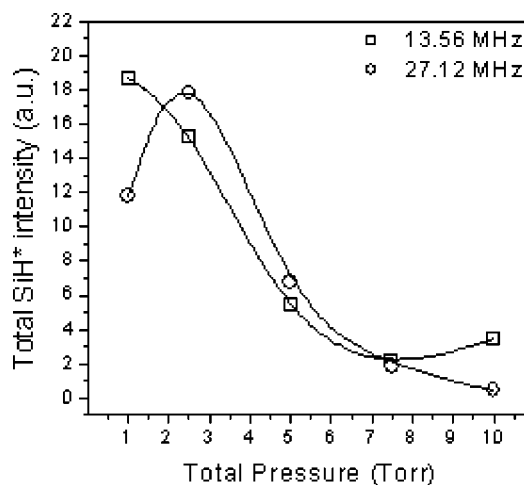


FIG. 5. Total SiH^* emission intensity as a function of the total gas pressure for the frequencies of 13.56 and 27.12 MHz.

the electron temperature. In any case these studies were not performed under constant power conditions and therefore their observations include an undetermined increase of power consumption with pressure leading to an enhancement of emission with an unknown trend.

The spatial distribution and the total species production presented so far indicate clearly that in general both frequency and pressure affect the spatial generation of radicals in a manner that does not favor the deposition rate. Namely, they both displace the maximum rate of production further from the substrate [Figs. 4(a) and 4(b)] and this is more definite in the high frequency, high pressure case. However, these changes of the spatial distribution and the total production of SiH^* species will affect the deposition rate only to the measure dissociative excitation towards SiH^* can be used to also represent the much lower threshold (8.4 eV) primary electron induced dissociation of SiH_4 towards free radicals. Some indirect information about this issue can be extracted from mass spectrometric measurements presented in the next section.

C. Mass spectrometry

SiH_4 consumption was measured using mass spectrometry under the same conditions. Figure 6 summarizes the results of these measurements as a function of the total gas pressure at 13.56 and 27.12 MHz. At 27.12 MHz the increase of pressure from 1 to 2.5 Torr leads to an important enhancement of the SiH_4 consumption from $\sim 15\%$ to 35% . A further increase up to 10 Torr, slightly favors SiH_4 consumption up to $\sim 42\%$. On the other hand, at 13.56 MHz, SiH_4 conversion is almost linearly increasing with pressure however the highest value is achieved is $\sim 32\%$ at 10 Torr. The observed low silane consumptions either at 13.56 or 27.12 MHz at any pressure do not confirm the term "silane depletion regime" in capacitive discharge conditions (i.e., in the absence of particles). It should be noted that the constant 72 mW/cm^2 power level was chosen as the highest possible power allowing for particle-free operation over the entire pressure range. This power level (or the particle-free operation regime) is of course responsible for the limited silane

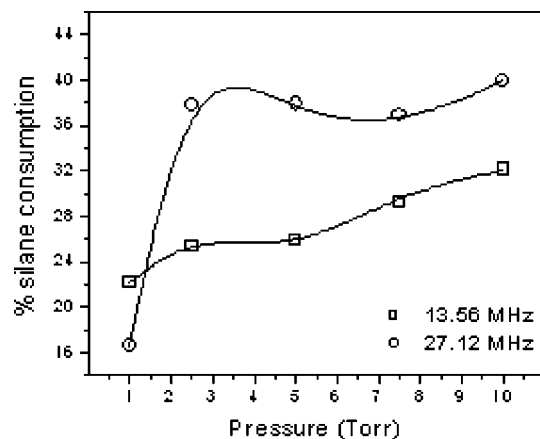


FIG. 6. % SiH₄ consumption as function of the total gas pressure for the frequencies of 13.56 and 27.12 MHz.

consumption. However, before deciding if this is a low power level one has to consider the relation of the accurately measured discharge power to the nominal (generator output) power. This power increases with pressure from 19 to 36 W (168–320 mW/cm²) in order to maintain constant power dissipation in the discharge. These values are in a range with those reported in several publications concerning μ c-Si:H deposition. This clearly means that the use of high pressures does not necessarily result in SiH₄ depletion.

Concerning the effect of frequency, the SiH₄ consumption is always higher at 27.12 MHz compared to 13.56 MHz for gas pressures above 2.5 Torr. This is not the case for the pressure of 1 Torr where silane consumption is comparable or higher at 13.56 MHz. Furthermore, useful conclusions concerning the dissociation processes can be drawn. Namely, SiH₄ is consumed either by direct electron-impact dissociation and ionization or through secondary gas phase reactions. Thus, the increase of SiH₄ consumption with frequency can mainly be attributed to an enhancement of primary electron impact processes because secondary gas phase reactions are not directly affected by the increase of frequency. In the same sense, no certain conclusions can be extracted concerning the effect of pressure on SiH₄ consumption with pressure as both primary processes and secondary reactions are affected by pressure. Thus, the effect of pressure on the gas phase chemistry and transport will be examined in detail in Sec. IV.

D. Deposition rate

The deposition rate of μ c-Si:H measured in conditions of constant power and constant silane concentration while varying the gas pressure at two frequencies is shown in Fig. 7. Similar to the emission curves there is a maximum deposition rate obtained for the pressure of 2.5 Torr in both frequencies. Beyond this pressure the deposition rate drops to about 1 Å/s at 10 Torr. Similar features were reported in previous works concerning the issue,^{13,26,27,33} although with a different optimal pressure. This discrepancy is certainly due to the different experimental conditions. In these papers the SiH₄/H₂ flow ratio is kept constant instead of silane partial pressure. However, the pressure at which the maximum is

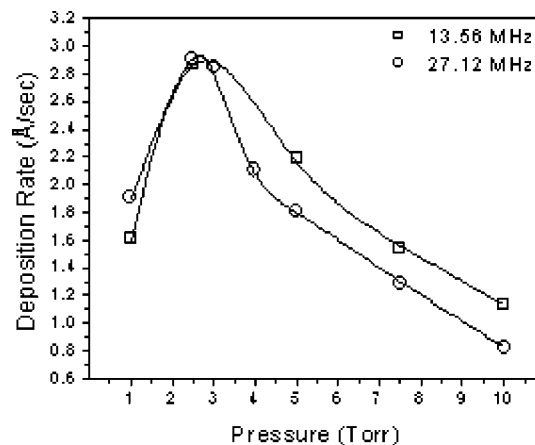


FIG. 7. Deposition rate of microcrystalline silicon as a function of the total gas pressure for the frequencies of 13.56 and 27.12 MHz.

observed depends on silane concentration and therefore would be shifted for another silane partial pressure. One may also argue that in these works, as mentioned in Sec. III B, there is also an undetermined power effect, whereas it is not certain that the experiments are performed in the capacitive regime.

It is worth nothing that a similar effect of pressure on the deposition rate was observed in experiments performed with different electrode gaps. Namely, there is always a maximum located at 2.5 Torr, however the effect of pressure is relatively smoother or more intense for lower and higher gaps, respectively.⁴²

Furthermore, the increase of frequency has a beneficial effect on the deposition rate only in the case of 1 Torr, whereas in all the other pressures there is no clear advantage of using 27.12 MHz. In fact, for pressures above 5 Torr, the deposition rate at 13.56 MHz exceeds slightly that of 27.12 MHz. At 2.5 Torr, where the maximum deposition rate is recorded, there is almost no difference between the two frequencies. This is inconsistent with most of the previous studies,^{13,20,28} showing an enhancement of the deposition rate under the combined increase of pressure and frequency, for the same reasons mentioned in the previous paragraph.

As a result, the total gas pressure has a dominant effect on the film growth rate leading to an increase that can reach up to 65% between 1 and 10 Torr. On the other hand, the increase of frequency in this pressure region does not affect the deposition rate as clearly as it affects the electrical characteristics and the consumption of silane presented above. Moreover, the results concerning the deposition rate are not related to SiH₄ conversion in a straightforward manner. Namely, at 1 Torr where SiH₄ consumption is higher at 13.56 MHz the deposition rate is lower compared to 27.12 MHz. For pressures higher than 1 Torr, where SiH₄ conversion is clearly favored at 27.12 MHz the deposition rate is not affected and for higher pressures drops at the higher frequency. On the other hand, the deposition rate is better related to the results of SRES, especially in the case of 27.12 MHz where an optimum on the total emission intensity was found at 2.5 Torr. In addition, the displacement of the maximum rate of production far from the substrate,

which was observed from the increase of both frequency and pressure, is also consistent with the drop of the deposition rate for pressures higher than 2.5 Torr. However, the emission curves and the deposition rate are not related at 13.56 MHz, especially concerning the absence of an emission maximum. Possible reasons for the existence of the optimum and for the pressure and the frequency effect on the deposition rate are presented in Sec. IV.

IV. DISCUSSION

The basis of this investigation is the choice to perform the experiments in conditions of constant discharge power while maintaining at the same time constant silane partial pressure. This choice has led to a combination of operating voltage, current, and phase impedance as presented in Sec. III A. However, these electrical characteristics are linked with electron properties like number density, energy, drift velocity, and collision frequency, quantities that are significantly altered while the power consumption is maintained constant. Among these, the effect of pressure and frequency on the electron density can be estimated if one examines the variation of the ohmic part of plasma impedance. The space averaged electron density n_{AV} and the discharge resistance R are related as follows:^{24,48}

$$n_{AV} = \frac{\nu_m d_b m_e}{RAe^2} = \frac{\nu_m d_b m_e I_d}{V_e \cos \phi A e^2}, \quad (1)$$

where m_e is the electron mass, d_b is the bulk length, A the discharge cross section, e the electron charge, ν_m the electron momentum transfer collision frequency, V_e , I_d , and ϕ the voltage amplitude, the discharge current, and the phase difference between them, respectively. The momentum transfer collision frequency was estimated using a Boltzmann equation solver,⁴⁹ which gives a value of $\sim 5 \times 10^9 \text{ Torr}^{-1} \text{ s}^{-1}$ for all the gas mixtures used in this study. In addition, the whole interelectrode space (15 mm) was taken as d_b mainly because in these high pressure conditions ohmic heating in the sheaths and its contribution to the discharge resistance is very important. Figure 8 shows the calculated average electron density as a function of the total gas pressure. A different behavior is observed at each frequency. Namely, the increase of pressure at 13.56 MHz gives an optimum electron density at 2.5 Torr. The lower electron density is calculated for the pressure of 1 Torr while the increase of pressure above 5 Torr has almost no effect on the plasma density. On the other hand, at 27.12 MHz there is a slight enhancement of electron density with pressure up to 7.5 Torr followed by a small drop at 10 Torr. The increase of pressure at 13.56 MHz can give an up to 50% increase while at 27.12 MHz the differences in electron density never exceed 30%. In any case, the electron density is higher compared to 13.56 MHz at any pressure and the difference is more important at higher pressures. This is consistent with many published results on the effect of frequency in gas discharges.^{21,22,24}

Moreover, from the electron density calculations one can also estimate the electron energy, taking into account that most of the power in these discharges is dissipated by elec-

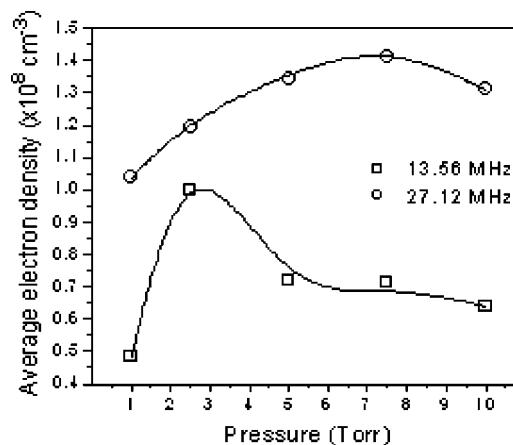


FIG. 8. Space-averaged electron density as a function of the total gas pressure for the frequencies of 13.56 and 27.12 MHz.

trons, the power consumed by ions being negligible at these low voltage conditions.^{24,50} The average energy gained/lost by electrons can be easily found by dividing the total power to the average electron density. Since the total power is maintained constant, electron energy will drop with the increase of frequency and will present its highest value for the 13.56 MHz, 1 Torr case. As an illustration, the estimated average energy per electron will be 4.5 eV for 13.56 MHz, 1 Torr, and 1.1 eV for the same pressure at 27.12 MHz.

It is normal that these changes in both the electron density and energy will strongly affect all electron–impact SiH_4 and H_2 processes and in particular those requiring high energy electrons. This has already been observed in Sec. III B, where the effect of pressure on the total SiH^* species production was presented. Namely, the differences observed depend directly on the evolution of the effective electron densities for this process at the two frequencies. However, the significant drop of emission intensity above 5 Torr at both frequencies, especially at 27.12 MHz, cannot be explained by the electron density changes, indicating that quenching of excited species also plays a role here.

Besides the electron properties that will strongly affect the rate of silane dissociation of SiH_4 and H_2 , there are important changes in the mass transport of precursors with pressure. In particular in the conditions examined here, where there is a wide variation of pressure while maintaining a constant total mass flow, an estimation of the changes of the gas flow regime is required. For this purpose, the main parameters involved in the mass transport of species like the diffusivity of species, the gas mixture velocity, as well as the Reynolds and Pecklet criteria, were calculated. The diffusion coefficient was calculated for SiH_4 in the binary mixture with H_2 according to the Chapman–Enskog theory,⁵¹ whereas the Pecklet number $[\text{Pe} = (u \cdot d) / D_{\text{SiH}_4}]$ (where u is gas velocity, d electrode gap, and D_{SiH_4} silane diffusion coefficient) was computed in terms of the SiH_4 diffusion coefficient. The Reynolds number $[\text{Re} = (u \cdot d \cdot \rho) / \mu]$ (where ρ is gas density and μ binary mixture viscosity) was calculated by again using the interelectrode space as the characteristic length. The results are summarized in Table I, where the mean residence time of SiH_4 is also included. As anticipated, the increase of

TABLE I. SiH₄ diffusion coefficient in the SiH₄/H₂ mixture (D_{SiH_4}), gas mixture velocity (u), Pecklet (Pe), and Reynolds (Re) numbers, mean SiH₄ residence time ($\bar{\tau}$) and time required for 90% of SiH₄ molecules to leave the reactor (τ_{90}) at five different gas pressures.

Pressure (Torr)	D_{SiH_4} (cm ² /s)	u (cm/s)	Pe	Re	t (s)	t_{90} (s)
1	1014	16.12	0.023	1279	0.093	13
2.5	428	6.45	0.0226	517	0.23	34
5	218	3.22	0.0221	259	0.46	70
7.5	146	2.15	0.0220	173	0.69	105
10	110	1.61	0.0219	129	0.93	141

pressure result in a significant reduction of both SiH₄ the diffusion coefficient and the gas flow velocity. The drop of these two parameters decreases the Pecklet number, which anyhow has rather small values, indicating that diffusion is still the main transport mechanism of species in the reactor even at the highest pressure used here. Thus, in the present conditions the cell behaves like a perfectly stirred tank reactor, which in turn ensures a uniform distribution of SiH₄ and H₂ although a single point gas entrance is used instead of a showerhead. This, combined with the low SiH₄ consumption (Fig. 6), ensures that there is no significant error in the correlation of plasma parameters and especially SRES data with the deposition rate. In fact, the increase of pressure for the same volumetric gas flow favors diffusion relative to convection leading to a significant suppression of the mass transport of species. In addition, the Re number drops significantly with pressure. Thus, for pressures higher than 2.5 the flow is laminar, while at 1 Torr is in the intermediate regime.

Moreover, the mean residence time of the gas mixture in the reaction space increases with pressure. However, the calculations of the Pe number have clearly showed that the reactor is far from the ideal plug flow or perfectly stirred reactor models. From this point of view, the mean residence time is meaningless; the parameter of interest being the distribution of the species residence time. Thus, in order to have a better estimation of the effect of pressure on the SiH₄ residence time, the model of dispersed axial flow was applied.⁵² According to this model, the fraction Φ of SiH₄ molecules that leave the discharge at time τ is given by the relation:

$$\Phi(\tau) = \frac{C}{C_0} = \frac{1}{2} \left[1 - \operatorname{erf} \left(\frac{\sqrt{\text{Pe}}}{2} \frac{1 - (\tau/\bar{\tau})}{\sqrt{\tau/\bar{\tau}}} \right) \right], \quad (2)$$

where C is the concentration of SiH₄ at the reactor's exit at time τ , C_0 is the initial SiH₄ concentration in the reactor, and $\bar{\tau}$ the mean residence time. Thus, the increase of the calculated SiH₄ residence time with pressure is shown in Fig. 9. According to these calculations the time required for 90% of the SiH₄ molecules (Table I, t_{90} and arrow in Fig. 9) to leave the reactor at 1 Torr is 13 s, while at 10 Torr it becomes 141 s. This is extremely high compared to the mean residence time and it clearly reflects the deviation of the plasma reactor from ideal plug flow reactors. The main reason for this rather high residence time is the significant domination of diffusion over convection that favors back mixing, radial diffusion, and trapping of molecules in the reactor. It also

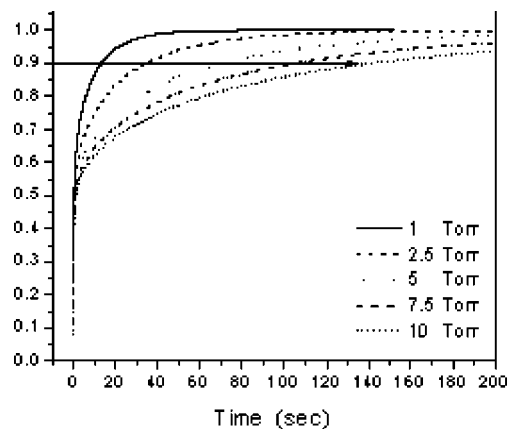
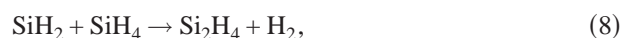
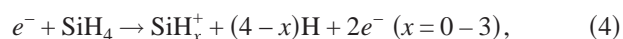


FIG. 9. Fraction of SiH₄ molecules leaving the discharge $\Phi(\tau)$ as a function of the time τ elapsed from their entrance.

worth noting that similar results are obtained if one uses the N-in series continuous stirred reactor (CSTR) reactors model instead of the axial dispersion model.

The fact that a large number of SiH₄ molecules leave the reactor at times much longer than the mean residence time will affect SiH₄ conversion which will normally increase with pressure. This has been already observed in Sec. III C, however a more detailed analysis of the gas phase chemistry of SiH₄/H₂ discharges is proposed.

The main reactions that are expected to contribute to the consumption of SiH₄ in the case of highly diluted SiH₄ in H₂ discharges are:



In order to distinguish between SiH₄ conversion due to electron impact dissociation (3) from that in ion/radical-SiH₄ reactions (6)–(10) a mass transfer model, described in detail in a previous work of this group,⁵³ was used. Briefly, the one-dimensional model simulates SiH₄/H₂ discharges in a parallel plate reactor taking into account plasma-surface interaction besides gas phase chemistry. The model inputs are the total SiH₄ consumption, calculated from the mass spectrometric measurements, and the spatial distribution of silane electron induced dissociation that is simulated by the SiH($A^2\Delta$) emission profiles (Fig. 4). The results of the model are the SiH₄ electron induced dissociation rate, the density distribution of various species in the discharge, the radical flux towards surfaces, and the deposition rate.

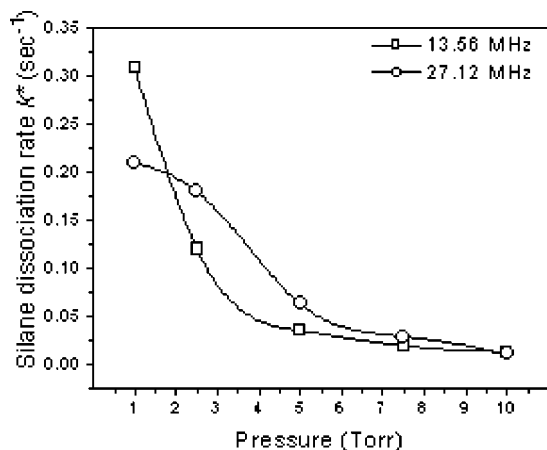


FIG. 10. Rate of SiH_4 electron-impact dissociation as a function of the total gas pressure for the frequencies of 13.56 and 27.12 MHz.

Application of the model to the present experimental conditions has led to the calculation of the electron impact SiH_4 dissociation rate k^* as presented in Fig. 10. Actually, k^* is the product of the electron-energy dependent rate constant multiplied by the average electron density and therefore is the electron- SiH_4 collision frequency leading to dissociation towards free radicals. The increase of pressure leads to a continuous drop of the SiH_4 dissociation rate for both frequencies. This drop is more pronounced in the region between 1 and 5 Torr and especially at 13.56 MHz. The dissociation rate is higher at 1 Torr, 13.56 MHz, while in all the other pressures is lower or about equal to the same one at 27.12 MHz. Furthermore, there are two important observations that have to be made concerning the variation of k^* with pressure and frequency. First, the values of k^* correspond to electron-silane collision times that are higher than the mean residence time and within the range of the SiH_4 residence times presented in Fig. 9. The second observation is that the variation of electron impact SiH_4 dissociation rate does not follow the evolution of the deposition rate (Fig. 7). Thus, despite the fact that at 1 Torr the rate of radical production is higher, the diffusive precursor fluxes towards the surfaces will be favored compared to any other pressure (Table I, diffusion coefficient) and the probability to reach the surfaces is enhanced [spatial distribution of species, Figs. 4(a) and 4(b)] the deposition rate is optimized at 2.5 Torr. This leads to the conclusion that the production of radicals through secondary gas phase reactions plays a very important role in these conditions and is determining the film growth rate. In order to further analyze this role, the total SiH_4 conversion X_{SiH_4} was written as the sum of the consumption due to each one in the group of parallel reactions (3)–(10): $X_{\text{SiH}_4} = \sum_{i=1}^8 X_i$, where, X_{3-10} corresponds to the conversion due to (3)–(10) respectively. The values of X_{3-10} can then be calculated using their rate constants and the residence time of SiH_4 . For instance the electron molecule collision processes are treated as first order reactions and the conversion X_1 can be calculated as

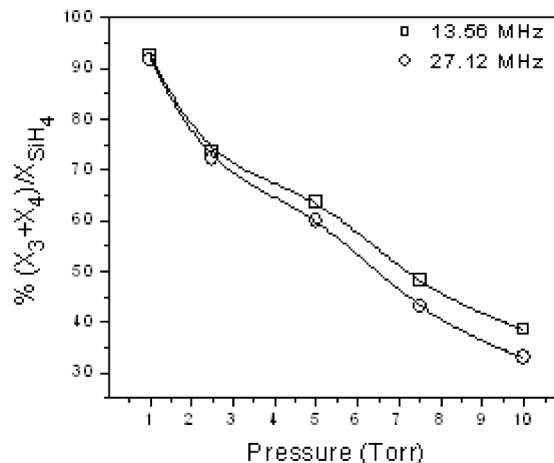


FIG. 11. Fraction of SiH_4 conversion due to primary electron- SiH_4 collisions $[(X_3+X_4)/X_{\text{SiH}_4}]$ as a function of the total gas pressure for the frequencies of 13.56 and 27.12 MHz.

$$X_3 = \int_0^{\infty} (1 - e^{-k^* \tau}) \Phi(\tau) d\tau = \int_0^1 (1 - e^{-k^* \tau}) d\Phi(\tau). \quad (11)$$

Thus, Fig 11 shows the fraction of SiH_4 consumption due to electron impact (X_1+X_2) as a function of the total gas pressure for the two frequencies. The increase of pressure leads to a drop of the relative importance of primary electron- SiH_4 impact reactions to the total SiH_4 conversion, for both frequencies. Namely, at 1 Torr the contribution of (3) and (4) to the total consumption is about 90% the rest being left to secondary reactions. This means that the process mechanism is simpler in this case, i.e., silicon based free radicals and ions are mostly produced through electron- SiH_4 collisions and they are lost to the surfaces (substrate, rf electrode, walls) due to diffusion or drift in the field. However, Fig. 7 shows that this is not the most favorable scheme for the film growth rate. In addition, these conditions do not favor film crystallinity since the films deposited at 1 Torr had the lowest crystalline volume fraction compared to all other pressures.⁵⁴ Namely, the crystallinity of the films, as estimated by laser Raman spectroscopy, was 75% at 1 Torr and $\sim 85\%$ for all the other pressures.

On the other hand, at pressures higher than 5 Torr and for both frequencies, secondary gas phase reactions start to play an equal or even a major role, participating by more than 50% to the total SiH_4 consumption. Under these conditions, radicals and ions initially produced (3) and (4), have the chance to further react with SiH_4 (7)–(10) due to the decrease of the rate that they reach the surfaces and the increase of SiH_4 residence time (Fig. 9). Furthermore, the reactions of hydrogen atoms and ions with SiH_4 (5) and (7) are also favored from the pressure increase for the same reasons, giving in such a manner to the secondary gas phase reactions the major role in the total SiH_4 consumption. Therefore, at higher pressures the deposition mechanism becomes more complicated, i.e., the film precursors are some free radicals (3) that escape from secondary reactions and mainly of radicals produced from secondary reactions (6) and (8)–(10).

Nevertheless, also this mechanism, where the precursors come mainly from the radical/ion-SiH₄ reactions, is not the most advantageous for the achievement of fast growth rates. In fact, at 10 Torr where the contribution of secondary reactions to the total conversion is about 65% the lowest deposition rates were recorded.

Finally, there is a pressure region between 2.5 and 5 Torr where electron-induced SiH₄ dissociation/ionization is still the main mechanism of SiH₄ conversion (60%–70%) while secondary reactions cannot be neglected as in the 1 Torr case. As shown again in Fig. 7, this combination gives the best results from the deposition rate point of view. The clear advantage of the limited participation of secondary gas phase reactions on the deposition mechanism can be better understood if one compares the results concerning the 1 and 5 Torr cases. The rate of free radicals production at 1 Torr, 13.56 MHz is about 1 order of magnitude higher than the corresponding 5 Torr one (Fig. 9), while the flux of these species towards the surface is more favored at the lower pressure. However, the deposition rate is higher at 5 Torr and this can only be due to the additional production of film precursors through secondary reactions. This additional source of precursors, together with the relatively high SiH₄ dissociation and the limited hindering of radicals fluxes to the substrate, leads finally to the observed optimum of the deposition rate at 2.5 Torr, for both frequencies.

The identification of the radicals responsible for the significant increase of the film growth rate is unambiguously an important subject of investigation. The model used here predicts that Si₂H₄ is mostly favored (8) by the controlled contribution of secondary reactions to the total SiH₄ conversion at the intermediate pressure. However, this result depends on the branching ratio of (3) and the sticking coefficient of this radical to the surfaces, which are both unknown. SiH₃ and Si₂H₅ are also species that will be enhanced through reactions (6) and (9), but in order to be considered as responsible for the observed increase of the deposition rate must have sticking coefficients much higher than the one (0.1) usually reported in the literature.^{55,56} In addition, the formation of silicon ion hydrides and especially of SiH₃⁺ is favored by secondary reactions (5) and (10) but the mechanism of ion incorporation as well as their precise role in the film growth is another interesting subject for research. Finally, concerning the role of hydrogen atoms in $\mu\text{c-Si:H}$ growth, the model predicts that hydrogen atoms dominates the flux of all the species (more than 1 order of magnitude higher than silicon hydrides) over the entire range of pressures. For the lowest pressure (1 Torr) the hydrogen atoms flux is enhanced relative to all other species due to the higher diffusion coefficient and the limitation of their consumption through the silane insertion reaction. This could increase the importance of silicon etching by hydrogen atoms at 1 Torr. However, the specific weight of this process on the deposition rate depends on the probability of hydrogen to extract a silicon atom from the surface and the values found in literature vary a lot. For instance, if one uses the probability proposed in Ref. 57 then H atom etching is of minor importance.

On the other hand, if the probability proposed by Tserapi *et al.*⁵⁸ is used then the observed drop of the deposition rate at 1 Torr is determined by etching.

V. CONCLUSIONS

An investigation of the total gas pressure (1–10 Torr) effect on the deposition of microcrystalline silicon thin films from highly diluted SiH₄ in H₂ discharges was carried out at the frequencies of 13.56 and 27.12 MHz. The study was based on the application of a series of plasma diagnostics together with a gas phase and surface simulator of SiH₄/H₂ discharges in conditions of constant rf power consumption in the discharge and at the same time constant silane partial pressure.

The achievement of constant power dissipation in the discharge has led to a minimum excitation voltage for the pressure of 2.5 Torr. The increase of pressure from 1 to 10 Torr is associated with a continuous drop of the discharge current and a monotonic displacement of the discharge phase to less negative values, for both frequencies. These changes of the discharge electrical parameters show a clear effect of pressure and frequency on the electron density. Namely, the increase of pressure results in a sharp optimum of electron density at 2.5 Torr for the 13.56 MHz case and to a weaker maximum at 7.5 Torr for the 27.12 MHz case. The electron energy is expected to follow an inverse relation to electron density as the total energy transferred to the plasma is maintained constant.

Moreover, the changes of the electron density and energy affect the rate of electron-SiH₄ impact processes that are mostly favored at lower pressures (1 and 2.5 Torr) for both frequencies. In addition, SRES measurements have shown that the increase of pressure displaces the maximum rate of species production far from the substrate, thus affecting the process in a manner that does not favor the film growth.

On the other hand, the % SiH₄ consumption is enhanced with pressure and is higher at 27.12 MHz; however, despite the rather high pressures, is far from depletion. The increase of SiH₄ conversion is attributed to the increase of SiH₄ residence time in the reactor and the consequent enhancement of the contribution of secondary gas phase reactions to the total SiH₄ conversion.

Finally, the deposition rate was found to present a clear optimum at 2.5 Torr and to be almost the same for 13.56 and 27.12 MHz, indicating that there is no clear advantage of using a combination of high pressure and frequency for the achievement of high $\mu\text{c-Si:H}$ deposition rate. The existence of this optimum was further analyzed, revealing that at these conditions the maximum of the film growth rate appears at the pressure where the SiH₄ dissociation rate to free radicals is rather high, while the fluxes of species to the surfaces are not significantly hindered and the secondary gas phase reactions act mainly as a source of additional film precursors. It should be noted that these conclusions are valid for the capacitive regime of operation where the presence of particles is excluded as in the case of the experiments presented here.

Further work is needed for the identification of the radi-

cals responsible for the significant increase of the film growth rate and the elucidation of the mechanism of ion incorporation.

ACKNOWLEDGMENTS

Two of the authors (E. Amanatides and D. Mataras) wish to thank the European Social Fund (ESF). Operational Program for Educational and Vocational Training II (EPEAEK II), and particularly the Program PYTHAGORAS for funding this work.

- ¹N. Wyrch *et al.*, Proceedings of the 2nd World Conference on Photovoltaic Energy Conversion, edited by J. Schmidt *et al.* (European Commission, Ispra, IT, 1998), Vol. I, pp. 467–471.
- ²K. Saito, M. Sano, K. Matsuda, T. Kondo, T. Nishimoto, K. Ogawa, and I. Kajita, Proceedings of the 2nd World Conference on Photovoltaic Energy Conversion, edited by J. Schmidt *et al.* (European Commission, Ispra, IT, 1998), Vol. I, pp. 351–354.
- ³J. Meier, R. Flückiger, H. Keppner, and A. Shah, Appl. Phys. Lett. **65**, 860 (1994).
- ⁴K. Yamamoto, M. Yoshimi, T. Suzuki, Y. Tawada, Y. Okamoto, and A. Nakajima, Mater. Res. Soc. Symp. Proc. **507**, 131 (1998).
- ⁵R. Schroop and M. Zeman, *Amorphous and Microcrystalline Silicon Solar Cells* (Kluwer Academic, Dordrecht, 1998).
- ⁶M. Tzolov, F. Finger, R. Carius, and P. Hapke, J. Appl. Phys. **81**, 7376 (1997).
- ⁷P. Torres, H. Keppner, J. Meier, U. Kroll, N. Beck, and A. Shah, Phys. Status Solidi A **163**, R9 (1997).
- ⁸A. Matsuda, J. Non-Cryst. Solids **338–340**, 1 (2004).
- ⁹U. Kroll, J. Meier, A. Shah, S. Mikhailov, and J. J. Weber, J. Appl. Phys. **80**, 4971 (1996).
- ¹⁰E. Amanatides, D. Mataras, and D. E. Rapakoulias, J. Vac. Sci. Technol. A **20**, 68 (2002).
- ¹¹D. G. Moon, B. H. Jung, J. N. Lee, B. T. Ahn, H. B. Im, K. S. Nam, and S. W. J. Kang, Mater. Sci. **5**, 364 (1994).
- ¹²U. Kroll, J. Meier, A. Shah, S. Mikhailov, and J. J. Weber, J. Appl. Phys. **80**, 4971 (1996).
- ¹³M. Kondo, M. Fukawa, L. Guo, and A. Matsuda, J. Non-Cryst. Solids **266–269**, 84 (2000).
- ¹⁴H. Curtins, N. Wyrch, and A. Shah, Electron. Lett. **23**, 228 (1987).
- ¹⁵F. Finger, R. Carius, P. Hapke, L. Houben, M. Luysberg, and M. Tzolov, Mater. Res. Soc. Symp. Proc. **452**, 725 (1997).
- ¹⁶S. Zhang *et al.*, J. Non-Cryst. Solids **338–340**, 530 (2004).
- ¹⁷C. Summonte, R. Rizzoli, E. Centurioni, D. Iencinella, L. Moretti, L. De Stefano, and I. Rendina, J. Non-Cryst. Solids **338–340**, 784 (2004).
- ¹⁸P. Delli Veneri, L. V. Merclodo, C. Minarini, and C. Privato, Thin Solid Films **451–452**, 269 (2004).
- ¹⁹E. Amanatides, D. Mataras, and D. E. Rapakoulias, J. Appl. Phys. **90**, 5799 (2001).
- ²⁰U. Graf, J. Meier, U. Kroll, J. Bailat, C. Droz, E. Vallat-Sauvain, and A. Shah, Thin Solid Films **427**, 37 (2003).
- ²¹T. Kitajima, Y. Takeo, N. Nakano, and T. Makabe, J. Appl. Phys. **84**, 5928 (1998).
- ²²M. Surenda and D. B. Graves, Appl. Phys. Lett. **59**, 2091 (1991).
- ²³M. Capitelli, C. Gorse, R. Winkler, and J. Wilhelm, Plasma Chem. Plasma Process. **8**, 399 (1988).
- ²⁴E. Amanatides and D. Mataras, J. Appl. Phys. **89**, 1556 (2001).
- ²⁵L. Sansonnens, A. A. Howling and Ch. Hollenstein, Plasma Sources Sci. Technol. **7**, 115 (1998).
- ²⁶L. Guo, M. Kondo, M. Fukawa, K. Saitoh, and A. Matsuda, Jpn. J. Appl. Phys., Part 2 **37**, L1116 (1998).
- ²⁷J. K. Rath, R. H. J. Franken, A. Gordijn, R. E. I. Schropp, and W. J. Goedheer, J. Non-Cryst. Solids **338–340**, 56 (2004).
- ²⁸M. Tanda, M. Kondo, and A. Matsuda, Thin Solid Films **427**, 33 (2003).
- ²⁹H. Aguas, P. Roca i Cabarrocas, S. Lebib, V. Silva, E. Fortunato, and R. Martins, Thin Solid Films **427**, 6 (2003).
- ³⁰S. Suzuki, M. Kondo, and A. Matsuda, Sol. Energy Mater. Sol. Cells **74**, 489 (2002).
- ³¹V. Suendo, A. V. Kharchenko, and P. Roca i Cabarrocas, Thin Solid Films **451–452**, 259 (2004).
- ³²Y. Fukuda, Y. Sakuma, C. Fukai, Y. Fujimara, K. Azuma, and H. Shirai, Thin Solid Films **386**, 256 (2001).
- ³³T. Takagi, R. Hayashi, G. Ganguly, M. Kondo, and A. Matsuda, Thin Solid Films **345**, 75 (1999).
- ³⁴M. Isomura, M. Kondo, and A. Matsuda, Sol. Energy Mater. Sol. Cells **66**, 375 (2001).
- ³⁵R. W. Collins and A. S. Ferlauto, Curr. Opin. Solid State Mater. Sci. **6**, 425 (2002).
- ³⁶T. Roschek, T. Repmann, J. Müller, B. Rech, and H. Wagner, J. Vac. Sci. Technol. A **20**, 492 (2002).
- ³⁷B. Rech, T. Roschek, T. Repmann, J. Müller, R. Schmitz, and W. Appenzeller, Thin Solid Films **427**, 157 (2003).
- ³⁸N. Spiliopoulos, D. Mataras, and D. E. Rapakoulias, J. Vac. Sci. Technol. A **14**, 2757 (1996).
- ³⁹N. Spiliopoulos, D. Mataras, and D. E. Rapakoulias, J. Electrochem. Soc. **144**, 634 (1997).
- ⁴⁰D. Mataras, S. Cavadias, and D. Rapakoulias, J. Appl. Phys. **66**, 119 (1989).
- ⁴¹E. Amanatides, S. Stamou, S. Boghosian, and D. Mataras, Proceedings of the 16th European Photovoltaic Solar Energy Conference, edited by H. Scheer *et al.*, (James & James Ltd., London, 2000), Vol. I, pp. 581–584.
- ⁴²E. Katsia, E. Amanatides, D. Mataras, and D. Rapakoulias, Proceedings of the 19th European Photovoltaic Solar Energy Conference, Paris, France, 3–7 July 2004, Vol. II, pp. 1601–1604.
- ⁴³M. Heintze, R. Zedlitz, and G. H. Bauer, J. Phys. D **26**, 1781 (1993).
- ⁴⁴A. A. Howling, J.-L. Dorier, Ch. Hollenstein, U. Kroll, and F. Finger, J. Vac. Sci. Technol. A **10**, 1080 (1992).
- ⁴⁵C. Beneking, J. Appl. Phys. **68**, 4461 (1990).
- ⁴⁶S. Tsurubuchi, K. Motohashi, S. Matsuoka, and T. Arikawa, Chem. Phys. **161**, 493 (1992).
- ⁴⁷F. Tochikubo, T. Makabe, S. Kakuta, and A. Suzuki, J. Appl. Phys. **71**, 2143 (1992).
- ⁴⁸V. A. Godyak, R. B. Piejak, and B. M. Alexandrovich, IEEE Trans. Plasma Sci. **19**, 660 (1991).
- ⁴⁹BOLSIG (Shareware), Kinema Software (<http://www.siglo-kinema.com/bolsig.htm>)
- ⁵⁰V. A. Godyak, R. B. Piejak, and B. M. Alexandrovich, J. Appl. Phys. **69**, 3455 (1991).
- ⁵¹R. B. Bird, W. E. Stewart, and E. N. Lightfoot, *Transport Phenomena* (Wiley, New York, 1960).
- ⁵²D. M. Himmelblau and K. B. Bischoff, *Process Analysis and Simulation: Deterministic Systems* (Wiley, New York, 1967).
- ⁵³E. Amanatides, S. Stamou, and D. Mataras, J. Appl. Phys. **90**, 5786 (2001).
- ⁵⁴E. Katsia, E. Amanatides, D. Mataras, A. Soto, and G. Voyiatzis, Sol. Energy Mater. Sol. Cells (submitted).
- ⁵⁵A. Matsuda and T. Goto, Mater. Res. Soc. Symp. Proc. **164**, 3 (1990).
- ⁵⁶J. Perrin, M. Shiratani, P. Kae-Nune, H. Videlot, J. Jolly, and J. Guillon, J. Vac. Sci. Technol. A **16**, 278 (1998).
- ⁵⁷J. Abrefah and D. R. Olander, Surf. Sci. **209**, 291 (1989).
- ⁵⁸A. Tserapi, J. R. Dunlop, B. Preppernau, and T. A. Miller, J. Vac. Sci. Technol. A **10**, 1188 (1992).